University of Wollongong
Research Online

Faculty of Science, Medicine and Health - Papers | Faculty of Science, Medicine and Health

2013

Accuracy of micrometeorological techniques for detecting a change in methane emissions from a herd of cattle

Johannes Laubach
Landcare Research NZ

Mei Bai
University of Wollongong, mb81@uow.edu.au

Cesar S. Pinares-Patino
Agresearch Grasslands Research Centre

Frances A. Phillips
University of Wollongong, francesp@uow.edu.au

Travis A. Naylor
University of Wollongong, naylort@uow.edu.au

See next page for additional authors

Publication Details

Laubach, J., Bai, M., Pinares-Patino, C. S., Phillips, F. A., Naylor, T. A., Molano, G., Cardenas Rocha, E. A. & Griffith, D. W. T. (2013). Accuracy of micrometeorological techniques for detecting a change in methane emissions from a herd of cattle. Agricultural and Forest Meteorology, 176 50-63.

Research Online is the open access institutional repository for the University of Wollongong. For further information contact the UOW Library: research-pubs@uow.edu.au

Accuracy of micrometeorological techniques for detecting a change in methane emissions from a herd of cattle

Abstract

Micrometeorological techniques are effective in measuring methane (CH4) emission rates at the herd scale, but their suitability as verification tools for emissions mitigation depends on the uncertainty with which they can detect a treatment difference. An experiment was designed to test for a range of techniques whether they could detect a change in weekly mean emission rate from a herd of cattle, in response to a controlled change in feed supply. The cattle were kept in an enclosure and fed pasture baleage, of amounts increasing from one week to the next. Methane emission rates were measured at the herd scale by the following techniques: (1) an external tracer-ratio technique, releasing nitrous oxide (N2O) from canisters on the animals' necks and measuring line-averaged CH4 and N2O mole fractions with Fourier-transform infra-red (FTIR) spectrometers deployed upwind and downwind of the cattle, (2) a mass-budget technique using vertical profiles of wind speed and CH4 mole fraction, (3) a dispersion model, applied separately to CH4 mole fraction data from the FTIR spectrometers, the vertical profile, and a laser system measuring along four paths surrounding the enclosure. For reference, enteric CH4 emissions were also measured at the animal scale on a daily basis, using an enteric tracer-ratio technique (with SF6 as the tracer). The animal-scale technique showed that mean CH4 emissions increased less than linearly with increasing feed intake. The herd-scale techniques showed that the emission rates followed a diurnal pattern, with the maximum about 2 h after the feed was offered. The herd-scale techniques could detect the weekly changes in emission levels, except that the two vertical-profile techniques (mass-budget technique and dispersion model applied to profile) failed to resolve the first step change. The weekly emission rates from the external tracer-ratio technique and the dispersion model, applied to data from either the two FTIR paths or the four laser paths, agreed within ±10% with the enteric tracer-ratio technique. By contrast, the two vertical-profile techniques gave 33–68% higher weekly emission rates. It is shown with a sensitivity study that systematically uneven animal distribution within the enclosure could explain some of this discrepancy. Another cause for bias was the data yield of the vertical-profile techniques being higher at day-time than at night-time, thus giving more weight to times of larger emission rates. The techniques using line-averaged mole fractions were less sensitive to the exact locations of emission sources and less prone to data loss from unsuitable wind directions; these advantages outweighed the lack of a method to calibrate CH4 mole fractions in situ.

Keywords

herd, emissions, methane, cattle, change, accuracy, detecting, techniques, micrometeorological, GeoQuest

Disciplines

Medicine and Health Sciences | Social and Behavioral Sciences

Publication Details

Laubach, J., Bai, M., Pinares-Patino, C. S., Phillips, F. A., Naylor, T. A., Molano, G., Cardenas Rocha, E. A. & Griffith, D. W. T. (2013). Accuracy of micrometeorological techniques for detecting a change in methane emissions from a herd of cattle. Agricultural and Forest Meteorology, 176 50-63.

This journal article is available at Research Online: http://ro.uow.edu.au/smhpapers/853

Authors
Johannes Laubach, Mei Bai, Cesar S. Pinares-Patino, Frances A. Phillips, Travis A. Naylor, German Molano, Edgar A. Cardenas Rocha, and David W. T Griffith

This journal article is available at Research Online: http://ro.uow.edu.au/smhpapers/853

Accuracy of micrometeorological techniques for detecting a change in methane emissions from a herd of cattle

Johannes Laubach[A,*], Mei Bai[B,**], Cesar S. Pinares-Patiño[C], Frances A. Phillips[B], Travis A. Naylor[B], German Molano[C], Edgar A. Cárdenas Rocha[C,D], David W. T. Griffith[B]

[A]*Landcare Research, P.O. Box 40, Lincoln 7640, New Zealand*

[B]*Centre for Atmospheric Chemistry, University of Wollongong, Wollongong NSW 2522, Australia*

[C]*AgResearch, Grasslands Research Centre, Tennent Drive, Palmerston North 4442, New Zealand*

[D]*Facultad de Medicina Veterinaria y Zootecnia, Universidad Nacional de Colombia, Carrera 45 No. 26-85, Bogotá, Colombia*

*Corresponding author:

Tel.: +64-3-321 9999

Fax: +64-3-321 9998

email: LaubachJ@LandcareResearch.co.nz

**present address: CSIRO Animal, Food & Health Sciences, Townsville QLD 4811, Australia

Submitted to Agricultural and Forest Meteorology 15 November 2012

Revised version, submitted 23 February 2013

Abstract

Micrometeorological techniques are effective in measuring methane (CH_4) emission rates at the herd scale, but their suitability as verification tools for emissions mitigation depends on the uncertainty with which they can detect a treatment difference. An experiment was designed to test for a range of techniques whether they could detect a change in weekly mean emission rate from a herd of cattle, in response to a controlled change in feed supply. The cattle were kept in an enclosure and fed pasture baleage, of amounts increasing from one week to the next. Methane emission rates were measured at the herd scale by the following techniques: 1) an external tracer-ratio technique, releasing nitrous oxide (N_2O) from canisters on the animals' necks and measuring line-averaged CH_4 and N_2O mole fractions with Fourier-transform infra-red (FTIR) spectrometers deployed upwind and downwind of the cattle, 2) a mass-budget technique using vertical profiles of wind speed and CH_4 mole fraction, 3) a dispersion model, applied separately to CH_4 mole fraction data from the FTIR spectrometers, the vertical profile, and a laser system measuring along four paths surrounding the enclosure. For reference, enteric CH_4 emissions were also measured at the animal scale on a daily basis, using an enteric tracer-ratio technique (with SF_6 as the tracer). The animal-scale technique showed that mean CH_4 emissions increased less than linearly with increasing feed intake. The herd-scale techniques showed that the emission rates followed a diurnal pattern, with the maximum about two hours after the feed was offered. The herd-scale techniques could detect the weekly changes in emission levels, except that the two vertical-profile techniques (mass-budget technique and dispersion model applied to profile) failed to resolve the first step change. The weekly emission rates from the external tracer-ratio technique and the dispersion model, applied to data from either the two FTIR paths or the four laser paths, agreed within ±10 % with the enteric tracer-ratio technique. By contrast, the two vertical-profile techniques gave 33 to 68 % higher weekly emission rates. It is shown with a sensitivity study that systematically uneven animal distribution within the enclosure could explain some of this discrepancy. Another cause for bias was the data yield of the vertical-profile techniques being higher at day-time than at night-time, thus giving more weight to times of larger emission rates. The techniques using line-averaged mole fractions were less sensitive to the exact locations of emission sources and less prone to data loss from unsuitable wind directions; these advantages outweighed the lack of a method to calibrate CH_4 mole fractions in situ.

Keywords: Cattle CH_4 emissions, Gas dispersion, Atmospheric surface layer, Tracer-ratio techniques, Mass-budget technique, Backward-Lagrangian stochastic model

1. Introduction

Methane (CH_4) emissions from ruminant livestock constitute about 30 % of New Zealand's and 12 % of Australia's greenhouse gas emissions. For any future practice or technology to mitigate these emissions, it must be verified at the “herd scale” (or “paddock scale”), under representative farming conditions, that the expected emissions reduction is achieved. In New Zealand (NZ) and Australia, cattle and sheep are farmed outdoors year-round. To measure CH_4 emissions outdoors, micrometeorological techniques are effective at the herd scale (Laubach et al., 2008). These can potentially verify small changes in emission rates, provided that the uncertainty with which such changes are detected is accurately known. Here, we report an experiment measuring the emissions from a herd of beef cattle that was designed to specify this uncertainty for a suite of micrometeorological techniques. These include: a mass-budget technique using vertical profiles of wind speed and CH_4 mole fraction ([CH_4]), a backward-Lagrangian stochastic (BLS) dispersion model using the same [CH_4] profiles, the same BLS model using line-averaged [CH_4] data gathered with two types of instruments, and an external tracer-ratio technique, releasing nitrous oxide (N_2O) co-located with the CH_4 emission sources and measuring line-averaged N_2O and CH_4 mole fractions upwind and downwind of the sources. The last technique was classified by Harper et al. (2011) as “non-micrometeorogical”, since it does not require any meteorological information to compute emission rates; however, as its feasibility relies on atmospheric transport, we consider it more appropriate to include it among the “micrometeorological” techniques. With these, it also shares the spatial and temporal scales at which it operates. To obtain non-micrometeorological reference values of CH_4 emissions on a daily basis, an enteric tracer-ratio technique was employed, commonly known as the SF_6 tracer-ratio technique. This technique operates at the “animal scale”, i.e. individual animals. Details and references for all techniques are given in later sections.

Laubach et al. (2008) already reported an experiment at the same site, with similar animals, and using the same techniques except for the external tracer-ratio technique. In that experiment, the animals were freely grazing in rectangular strips that were changed daily. This represented usual farming practice in NZ but had two disadvantages: the instrumentation had to be moved frequently to be in suitable locations for capturing the emissions, and the feed intake of the animals could not be measured. Knowing the feed intake is desirable because it is a major factor determining CH_4 emissions. The "methane yield" Y_m, defined as the ratio of CH_4 emissions per dry-matter intake (DMI) where both variables are expressed in units of combustion energy, is recommended for inventory purposes (IPCC, 2006; Lassey, 2007). To overcome the two disadvantages in the present experiment, the cattle were held in a grass-free area and were fed known quantities of pasture baleage. The experiment was run for three weeks. Within each week, daily feed rations were held constant, then increased for the following week in order to produce a measurable step change in the herd's CH_4 emissions. The objective was to test for each technique whether it was possible to detect this step change on the basis of weekly averages, which in turn required quantification of the uncertainty of these averages. Factors determining this uncertainty are not only measurement accuracy, but also for each technique its data yield, i.e. the number of runs meeting specific quality criteria, and its sensitivity to the spatial distribution of sources (which is always assumed homogeneous across a prescribed area, except for the external tracer-ratio technique, where no such assumption is needed).

A side issue, inadvertently discovered from consistency checks between the different CH_4 instruments, is a strong temperature dependence of the "GasFinder" CH_4 laser, previously unreported in the micrometeorological literature. This result is presented and empirically corrected for in the main text; the causes are discussed in the Appendix.

2. Experimental design

The experiment was conducted in November 2008. The site (40.336° S, 175.465° E) was located on the Aorangi Research Farm, ca. 20 km inland from the west coast of the North Island of NZ, near the city of Palmerston North. It is ideally suited for micrometeorological techniques and tracer dispersion studies because the surrounding terrain is flat for several km in all directions and there is a predominant wind direction, from W (which includes frequent afternoon sea breezes when synoptic winds are weak). The cattle were managed in two groups, of 30 and 31 animals, respectively, with identical treatments as described in 2.2.

2.1 Site preparation and setup geometry

A paddock area of about 200 m by 200 m had been sprayed with herbicide prior to the experiment, so that the ground was initially bare; by the end, a thin cover of herbage had grown back. In the NW quarter of this area, a rectangle of 80 m by 55 m was fenced to contain the cattle herd. A 7 m tall mast to collect vertical profiles of wind speed and CH_4 mole fraction was erected at the midpoint of the E boundary of the fenced area, and with additional fencing of a semicircle with 20 m radius, the cattle were kept at a minimum distance of 20 m from the mast. The nominal source area (rectangle minus semicircle) thus covered 3772 m^2. This area was subdivided into two equal-size enclosures (Fig. 1) to allow handling of the cattle in two separate groups and to limit clustering of the animals at feeding time.

The surrounding terrain consisted mainly of flat paddocks, with no significant flow obstacles to the W, S and E for at least 500 m. To the N, there was a water ditch dropping 2 m below ground level at 50 m distance from the profile mast, and a shelterbelt at ca. 150 m distance. The bare ground extended ca. 100 m from the mast to the W, S and E, and 45 m to the N.

Two types of line-averaging optical sensors (described below) were employed (Fig. 1). One was a CH_4-specific laser system with four paths that were mounted outside the cattle area, with one path along each side of the rectangle, at 5 to 10 m distance from the fence. Path lengths were between 53 and 57 m, measured with 0.1 m accuracy, and path heights above ground were 1.85, 1.37, 1.38 and 1.07 m (±0.02) m for the W, S, E and N path, respectively. The other instrument type was a Fourier-transform infra-red (FTIR) spectrometer, measuring mole fractions of multiple gas species simultaneously along an open path. Two identical FTIRs were set up parallel to the W and E sides of the rectangle, at about 5 and 12 m distance to W and E, respectively. The path lengths were 88.9 and 89.5 m and the heights above ground were 1.39 (±0.05) m.

Wind direction, atmospheric stability and velocity statistics (required as inputs for the dispersion model) were measured with a sonic anemometer (81000V, RM Young, Traverse City, Michigan, USA), mounted on top of a telescope mast, 3.85 m above ground and 13 m NNW of the profile mast.

2.2 Animals and feed

The experiment involved 61 one-year-old Friesian-Hereford crossbred steers. They were fed perennial ryegrass/white clover baleage that had been prepared on-farm, with an approximate content of white clover of 20 % (DM basis). The chemical composition of the feed was determined by near-infrared spectroscopy.

Prior to the start of measurements, the animals were acclimatised to the management conditions over a period of 10 d by gradually increasing the baleage fraction in the diet while decreasing herbage allowance. At the same time, the animals were accustomed to wear the gas collection gear required for the SF_6 tracer-ratio technique. Starting on the 6th day of acclimatisation, baleage constituted 100 % of the diet. The cattle were fed at three increasing feeding levels (low, medium and high) over three consecutive periods of one week duration each. The first three days of each week were considered as adjustment periods to the new feeding level, and the last four days were used to conduct CH_4 emissions measurements with the animal-scale technique. Feeding levels were set with the intention of making 1.0, 1.5, and 2.0 times maintenance energy requirements available to the steers during Weeks 1, 2 and 3, respectively. The maintenance energy requirement was estimated following CSIRO (2007). In order to allow for increasing fractions of feed wastage with increasing feeding level, the feed amounts offered were set to 1.10, 1.73 and 2.60 times maintenance requirements. The animals were weighed at the start of the experiment and at the end of each one-week feeding period. Drinking water was freely available to them, from troughs placed centrally in each enclosure.

The feed bales weighed around 450 kg. Every morning at 09:00 h the feed was distributed on the ground inside the two enclosures, using a forage mixer feed-out wagon equipped with a scale. The accuracy of the wagon's scale was calibrated against a load cell at the start of the experiment and found to agree within ±10 kg for a bale. In each enclosure, the feed was laid out approximately in a "B" shape, which maximised the areal spread of the feed while avoiding that the feed-out wagon had to cross the supply pipes to the water troughs (Fig. 1).

Estimation of feed intake on the basis of metabolisable energy algorithms was not considered reliable, because the 7 d long feeding period at each level was too short to accurately account for liveweight change due to the potentially overwhelming influence of variable gut fill when the animals were weighed. Alternatively, feed intake estimates were to be based on the difference between feed offered and refused. However, refusals were trampled and mixed with faeces and soil, and attempts to collect representative samples proved impractical. Consequently, the proportion of refused feed was estimated daily by visual assessment.

2.3 Profile mast instrumentation

The vertical profile of [CH_4] was measured with an analyser using off-axis integrated cavity output spectroscopy (DLT-100, Los Gatos Research, Mountain View, California, USA). Air was drawn continuously from seven intakes via tubes into ballast volumes. A datalogger-controlled valve-switching system sequentially selected each of the intake lines for sampling by the analyser. Each switching cycle lasted 20 min, allocating 171 s of sampling time to each intake, of which the first 140 s were discarded as flushing time to purge the sample cell of air from the previous intake. Five of the intakes were mounted on the mast, at heights of 0.62, 1.22, 2.24, 4.13 and 7.18 m (±0.02) m. The other two were placed to the W and SE away from the cattle area (Fig. 1), at 1.94 and 1.77 m height, respectively, so that for any wind direction one of them would be suitably located to provide the local background mole fraction (upwind of the herd).

Wind speed, relative humidity (RH) and temperature were measured at the same five heights as [CH_4]: wind speed by cup anemometers (A101M, Vector Instruments, Rhyl, Clwyd, UK) with matched calibrations, humidity by capacitive RH sensors (MP100A, Rotronic, Bassersdorf, Switzerland) and temperature by thermocouples inside the same aspirated double radiation shields as the RH sensors.

2.4 Open-path instrumentation

The four-path CH_4 laser system (GasFinder MC, Boreal Laser, Edmonton, Alberta, Canada) consists of a central control unit, four remote heads (Fig. 2a) and four retro-reflectors. The central unit houses the laser source, of wavelength 1653 nm, a sealed reference cell filled with a known amount of CH_4, an optical multiplexer and the controlling and processing electronics. The wavelength is modulated across a narrow band in order to sample the shape of the absorption line. The IR light is ducted via fibre-optical cables to the remote heads, switching between them in a cycle of ca. 18 s duration. The head emits the light along the open path towards the retro-reflector and collects the returning light on a photodiode. The electrical output signal of the photodiode is transmitted back to the central unit via a coaxial cable. There, the light intensity measurements, as scanned across the waveband, are converted to CH_4 mole fractions with a regression algorithm that compares the measured line shape to that of the reference cell (Boreal Laser, 2005). These mole fraction data were collected on a laptop computer and subjected to post-processing to remove dubious data (guided by quality flags and light level data provided by the instrument), apply correction factors for signal dampening along the coaxial cable length, and form 20-min averages aligned with the switching cycles of the vertical profile system.

The two identical open-path multi-gas FTIR spectrometer systems were constructed at the University of Wollongong (Bai, 2010). The spectrometer is a Matrix-M IRcube (Bruker Optik, Ettlingen, Germany). Light from an air-cooled SiC infrared source is modulated by the interferometer and passes via a beam splitter (ZnSe window) into a modified 10” Schmidt-Cassegrain telescope (LX200R, Meade Instrument Corp., Irvine, California, USA). From there, the primary beam is transmitted across the measurement path, returned by a 0.3 m diameter retro-reflector array (PLX, Deer Park, New York, USA) and received by a HgCdTe detector (Infrared Associates, Stuart, Florida, USA) which sits on the same tripod-mounted optical bench as the source, interferometer and telescope (Fig. 2b). A Zener-diode thermometer (type LM335) and a barometer (PTB110, Vaisala, Helsinki, Finland) are integrated in the source/detector array to provide real-time air temperature and pressure data for the analysis of the measured spectra. The spectrometer is controlled by software developed at the University of Wollongong. The interferometer performs about 80 scans min^{-1} across the waveband of interest ($700 – 5000\ cm^{-1}$), which were in this experiment averaged to 2-min spectra. From the spectra, the mole fractions of CH_4, N_2O, CO_2, CO and H_2O are retrieved by a non-linear optimisation algorithm (MALT software), developed by Griffith (1996). The algorithm uses absorption line strengths of these gases as listed in the HITRAN database (Rothman et al., 2005) and constructs the combination of mole fractions that provides the best match between the transmission spectrum expected from this combination and the observed spectrum (Smith et al., 2011; Griffith et al., 2012). Only the CH_4 and N_2O mole fractions are used in this experiment.

3. Techniques to determine CH_4 emission rates

The various techniques to determine the CH_4 emission rates are listed in Table 1. The first technique (Section 3.1) was applied to individual animals, providing daily averages. The others (Sections 3.2 to 3.4) all integrated over emissions from the herd, as the emitted CH_4 was transported and dispersed by the wind. They were applied using 20-min averages of the CH_4 mole fraction, relative to moist air, and of the meteorological variables.

3.1 Enteric tracer-ratio technique (SF_6)

The SF_6 tracer-ratio technique (Johnson et al., 1994) was employed to estimate CH_4 emissions from individual animals. For this purpose, on the first day of the pre-trial acclimatisation period of 10 d, individually calibrated brass permeation tubes containing the SF_6 tracer were dosed *per os* into the reticulo-rumen of each participating animal. For the last four days of each feeding level period, daily breath and background air samples were collected from each steer, using a yoke fitted around his neck (Fig. 3). Although the animals were out of the paddock for 2 to 3 h every morning (time spent in transit to and from the management yards and for handling), changing the sampling yoke took only about 1 min per animal, thus the collection period was effectively 24 h. Samples were transported to the laboratory for analysis of SF_6 and CH_4 mole fractions using a gas chromatograph (GC-2010, Shimadzu, Kyoto, Japan), as described by Pinares-Patiño et al. (2007). Daily CH_4 emissions from individual animals were calculated from the ratio of mole fraction elevations of CH_4 and SF_6 (above the respective background-air mole fractions) and the known permeation rate of SF_6 from the permeation tubes (Johnson et al., 1994).

3.2 External tracer-ratio technique (N_2O)

The basic approach of the N_2O tracer-ratio technique is the same as for the SF_6 technique: a tracer gas is released at a known rate co-located with the CH_4 emission from the animals, the mole fractions of both gases are measured post-emission in the same volume, and then the ratio of the two mole fractions (after subtracting atmospheric background from each) is equated with the ratio of their emission rates. The main difference is that with the N_2O technique the gases are not collected in a container, but measured in situ, some distance downwind, by the open-path FTIR. The path length is long enough to capture the emissions from many, if not all, animals simultaneously, which makes the technique effective at the herd scale. Along with this spatial integration comes high temporal resolution, not achievable with the animal-scale technique.

Nitrous oxide was chosen because it is inert, non-toxic, commercially available and its spectrum documented in HITRAN, which makes it easily measurable by the FTIR in the same wavebands as CH_4. Also, it could be released at rates much larger than from any environmental sources (soil and animal excreta), so that the measured downwind-upwind [N_2O] differences were clearly attributable to the manufactured release. In a previous experiment, Griffith et al. (2008) released the N_2O from a perforated pipe along the upwind fence line. Here, the release location was much more closely matched to that of the CH_4 by using pressurised canisters carried by the animals near their mouths (Fig 3). These were 12 oz paintball gas canisters (Catalina cylinders, Garden Grove, California, USA), which were filled with ca. 0.3 kg liquid compressed N_2O and fitted to the animals on a daily schedule, along with the SF_6 collection yokes to which they were attached. Due to the long preparation time required to fill the N_2O canisters, only half of the cattle (15 in each group) were equipped with them. This was unlikely to introduce additional error because animals with and without release canister distributed themselves randomly across the same area. Each canister was fitted with a tap and restricting orifice to regulate the release rate to about 10 g h^{-1}. The release rate's time average was determined for each canister by weighing it, before and after it was carried by the animal, and the release rate's temporal evolution was constructed by taking into account its systematic decrease with canister pressure as well as its temperature dependence. Technical details of the canister filling procedure and the computation of the N_2O release rate are given in Bai (2010). The CH_4 emission rate was then calculated from the total N_2O release rate and the path-integrated CH_4 and N_2O mole fractions measured downwind from the herd.

3.3 Micrometeorological mass-budget technique

The mass-budget technique, sometimes also named integrated horizontal-flux technique, was first applied to animal emissions by Harper et al. (1999) and Leuning et al. (1999). Here, it was implemented using the vertical 5-point profiles of CH_4 mole fraction, measured with the Los Gatos analyser, and of wind speed, measured with the cup anemometers. From these profiles and the background mole fraction, measured upwind of the cattle, the integrated horizontal flux of CH_4 was computed. To convert this flux to an areal emission rate, it was divided by the distance across the cattle area, from the profile mast in the upwind direction. Corrections for cross-wind variation of this distance, for horizontal flux contributions above the top measurement height, and for turbulent backflow were applied as described in Laubach and Kelliher (2004).

3.4 BLS technique

The principle of the backwards-Lagrangian stochastic (BLS) technique is to employ a dispersion model to simulate trajectories of air parcels backwards in time from a location where a gas concentration was measured, and to analyse statistically where these trajectories intersect with a source volume (or area) in which the concentration of the simulated air parcels would have been altered. For a given flow field (mean wind, direction, and certain turbulent parameters), this trajectory-mapping delivers an unambiguous linear relationship between measured concentration and emission rate.

The BLS model used here, developed by Flesch et al. (1995; 2004), is distributed as a user-friendly software (WindTrax 2.0, www.thunderbeachscientific.com). The model can accommodate concentration measurements at a point, such as realised by an intake to a gas analyser, or along a line, such as the path of an optical sensor measuring absorption. It is here applied separately to the three types of CH_4-measuring instruments: the closed-path analyser (vertical profile), the open-path laser system (4 paths) and the open-path FTIR instruments (2 paths). While the three simulations differ in their concentration input data, they assume identical CH_4 source distributions and identical flow fields. The CH_4 source is defined as a ground-level area source with the dimensions of the cattle enclosure. The flow field is specified, as in Laubach (2010), by wind speed from the highest cup anemometer, the stability parameter and the standard deviations of the three wind components from the sonic anemometer (at 3.85 m), and roughness length. Roughness length was not allowed to vary randomly from run to run; rather, its evolution for the whole experiment was determined as a function of time and wind direction. Over time, the roughness length increased slowly as vegetation grew back, from 0.8 cm (bare soil) to 1.7 cm. The directional analysis showed systematically larger values from the N sector than from the other directions, consistent with the presence of ditch and shelterbelt to the N. The directional dependence was fitted with a squared cosine function for directions within ±90 ° from N, added to the time-dependent roughness length for the other sectors. The maximum roughness length obtained for N winds was 9.1 cm.

4. Calibration checks and corrections to CH_4 mole fractions

4.1 Closed-path analyser

Every 6 h, sampling of vertical [CH_4] profiles with the closed-path analyser (Los Gatos) was interrupted for 20 min to perform an automated calibration check, using two gas cylinders that provided air with near-zero and near-ambient CH_4 mole fractions. These checks showed that throughout the campaign, [CH_4] was reproducible within ±3 ppb standard deviation (±0.18 % of ambient). Testing for temperature dependence, a linear regression slope of 0.07 ppb K^{-1} was found, which is a factor 12 smaller than reported by Tuzson et al. (2010) for the same type of instrument. With $R^2 = 0.03$, this temperature dependence was not significantly different from zero and thus neglected. Instead, the observed differences between subsequent calibration checks were used to correct the mole fraction data in post-processing, assuming a linear drift in time. Within a 20-min run, this drift correction had negligible effect on mole fraction differences between intakes, but it provided minor adjustments to the diurnal courses.

4.2 Open-path FTIR instruments

For the open-path instruments, in-situ calibration checks were not possible. Instead, a series of consistency checks was conducted, first between paths of the same system, then between these and the closed-path instrument. For these checks, only the periods of cattle absence were used, expecting that then all instruments would effectively sample the local background CH_4 mole fraction – not necessarily identical to hemispheric background, but influenced only by sources (or sinks) far enough away that the position differences between the compared instruments did not matter.

As the periods of cattle absence were in the morning, strongly stable stratification from the residual nocturnal boundary could occur on some days, with elevated CH_4 concentrations that potentially showed a vertical structure. To be able to identify the influence of stable versus well-mixed conditions, the [CH_4] data from the two FTIR instruments are compared by plotting their ratio as a function of the wind speed at 7.18 m (Fig. 4). As a change in alignment can change the instrument calibration, the data are split into two groups, before and after a realignment of the W path that was necessary following disturbance to the instrument while diagnosing an electronic failure. Before the realignment, the ratio was consistently near 1, except for some runs of low wind speed which are considered as stably stratified and not well-mixed. The mean (±SD) for wind speed > 2 m s^{-1} was 1.007 (±0.009, n = 67). After the realignment, the ratio was 1.034 (±0.006, n = 30). The SD values indicate a random error of order 5 to 10 ppb at ambient [CH_4]. This estimate would include an error contribution from the horizontal distance between the instruments; it is thus compatible with several independent instrument precision checks that yielded estimates between 2 and 4 ppb (Bai, 2010).

Similar tests were done for the N_2O mole fractions, required for the external tracer-ratio technique (not shown). These yielded W/E ratios of 1.02 (±0.01) before and 1.03 (±0.01) after realignment, respectively. The SD values indicate a random error of 2 ppb at ambient [N_2O], which again – due to the error from the horizontal separation – is compatible with independent precision checks, yielding 0.4 ppb (Bai, 2010).

To compare the two FTIR to the closed-path analyser, [CH_4] from each of the former was divided by [CH_4] from the nearest intake of the latter, selecting the same cattle-free periods as before. The nearest path for the W path FTIR was the background intake at 1.94 m height, and for the E path, the second-lowest intake from the profile mast, at 1.22 m height. Since the open-path and closed-path data differ in three respects: height, averaging volume (“line” vs. “point”), and sampling duration (shorter for closed-path due to the switching cycle), one should not expect perfect agreement. However the ratios showed remarkable consistency, at about 0.97 for the E path and about 0.98 and 1.01 for the W path before and after the realignment, respectively (±0.01 for each ratio). The ratios were independent of temperature and humidity. Any ratios less than 0.94 were associated with wind speed < 2 m s^{-1}. This indicates that the absolute mole fractions of the two FTIR instruments were 2 to 3 % too low, equivalent to an absolute error of 40 to 60 ppb at background, and they did not drift.

After these checks, the mole fractions from the W path were corrected against those from the E path, by factors determined as the slopes of period-wise linear regressions (of runs without cattle presence). This ensured matched calibrations between the two FTIRs, which are crucial for accurate determination of upwind-downwind differences, and in turn, emission rates. The FTIR data were not corrected against the closed-path data. Thus, it is expected that the 3 % difference between the E

FIR and the closed-path analyser carries through to the emission rate computations with the BLS technique.

4.3 Four-path laser system

For the open-path laser (GasFinder MC), the same consistency checks were carried out as for the FTIR. In Fig. 5, consistency between paths is assessed, by showing the ratios of [CH_4] from the W, S and N path, respectively, to [CH_4] from the E path, against wind speed. For each ratio, the spread is considerably larger than for the W/E FTIR ratio in Fig. 4, and wind speed does not affect the spread, indicating that the variability reflects instrument precision, not true [CH_4] variations. The means (±SD), for 126 runs of cattle absence, were 1.015 (±0.039) for W/E, 0.963 (±0.038) for S/E, and 1.033 (±0.041) for N/E, respectively. The SD values indicate a random error of order 48 ppb, at ambient [CH_4], for each path. This is compatible with the manufacturer's specification of 2 ppm m precision for the path-integrated mole fraction, equivalent to 36 ppb for a 55 m long path. The laser system is thus one magnitude less precise than the FTIR instruments and the closed-path analyser.

In Fig. 5, the differences of the mean ratios from 1 cannot be explained by height differences (the W path was the highest, N the lowest, and S and E were at equal height). Like for the FTIR, the E path was selected as the reference path, and the [CH_4] data from the other three paths were corrected against it. This was done separately for the three feeding-level periods, to ensure the [CH_4] differences between paths were bias-free within each such period.

As for the FTIR, mole fractions from the W and E paths of the laser system were compared to those from the nearest intakes of the closed-path analyser. Both horizontal and vertical distances between path and intake location were smaller than for the FTIR. Therefore, it was considered acceptable to include runs with and without cattle presence in the comparison. To ensure sufficient atmospheric mixing, only runs with wind speed > 2 m s^{-1} were selected. The path/intake [CH_4] ratios reveal a significant temperature dependence (Fig. 6), with a slope of -9.4×10^{-3} K^{-1} for both. The ratio equals 1 at 23 (±2) °C (equal to the reference temperature, 296 K, of the HITRAN database – see Appendix), while at 0 °C the open-path laser would overestimate [CH_4] by about 20 %. It was further tested whether the [CH_4] ratios depended on specific humidity or pressure, with negative result. This test was repeated with the data binned into 3 K wide temperature classes, to prevent that the temperature dependence would overwhelm any trends with the other variables, but no dependence on humidity or pressure could be identified. By contrast, when the data were binned into five classes of specific humidity, or pressure, then within each class there was still a temperature dependence, represented by a slope that agreed within ±30 % with that in Fig. 6. For all subsequent analyses, the [CH_4] data from the laser system are therefore linearly corrected for temperature, using the slope from Fig. 6 as the adjustment factor.

To our knowledge, such a temperature dependence of the GasFinder has not been reported in the micrometeorological literature before. Possible physical causes are discussed in the Appendix.

5. Results and Discussion

5.1 Animal behaviour

On the majority of mornings, the cattle were taken off-site between 7:15 and 8:00 h, to have their gas collection yokes changed. During their absence, the feed was laid out in the enclosures. When the cattle returned, between 10:00 and 10:30 h, they began feeding immediately, and used up the available rations within a few hours. The rest of the day they spent mostly drinking, resting and ruminating, moving around less than grazing animals typically would. It was clear from observations, of the cattle themselves as well as the distribution of their excreta, that they stayed preferably in the W parts of the enclosures, frequently bunching near the W fence line (and occasionally, around the water troughs). This behaviour was very different from the freely-grazing behaviour observed by Laubach and Kelliher (2004; 2005b) and Laubach et al. (2008), when the paddock area was by and large evenly covered by the cattle, for most of the time. The uneven spatial animal distribution in the present experiment had implications for the emission rate determinations. These are discussed in Section 5.5.

5.2 Feed intake and emission rates at the animal scale

On average, the baleage contained 399 (±26) g dry matter (DM) per kg wet weight. On a DM basis, it contained 46.5 (±5.5) % neutral detergent fibre, 19.0 (±3.4) % crude protein, 9.4 (±2.3) % soluble sugars, 3.3 (±0.5) % lipids and 13.8 (±3.0) % ash. The estimated metabolisable energy content of the feed was 10.5 (±0.4) MJ (kg DM)$^{-1}$.

The average liveweight (LW) of the cattle increased with level of feeding from 331 kg at low level to 352 kg at the high level (Table 2). On a DM basis, feed on offer increased by 58 % from the low to the medium level of feeding and by 52 % from the medium to the high level. Visual assessment of feed refused showed negligible amounts (< 1 %) for Weeks 1 and 2. In Week 3, the soiled feed residues were considerably larger and estimated at 10 %. The resulting estimates of dry matter intake (DMI) were 4.3, 6.7 and 9.3 kg DM d^{-1} $animal^{-1}$ for the low, medium and high feeding level, respectively (Table 2), and hence the relative increases from one feeding level to the next were 58 and 38 %, respectively.

The CH_4 emission rates were obtained with the SF_6 tracer-ratio technique, for the last 4 d of each week. The first 3 d were considered as an adjustment period to the new feeding level (as diet composition did not change and feeding level increased, rather than decreased, a period of 3 d sufficed). The average emission rates were 70.8 (±13.5), 89.7 (±11.1) and 119.1 (±16.4) g CH_4 d^{-1} $animal^{-1}$ for Weeks 1, 2 and 3, respectively (Table 2), where the numbers are means (± SD) of the 61 animals. Even in Week 3, when DMI was relatively generous, the CH_4 emission rate was low in comparison to those observed previously for freely-grazing steers at the same location (Laubach et al., 2008). The standard deviations in Table 2 convert to standard errors of the mean ≤ 2 g CH_4 d^{-1} $animal^{-1}$. We assume the weekly mean CH_4 emission rates to be "true" within this limit and use them as reference values for the other techniques. The accuracy of the SF_6 technique for estimating mean emissions of CH_4 has been proved by comparison to animal chamber measurements, both for sheep (Hammond et al., 2009) and cattle (Grainger et al., 2007).

The CH_4 emission rate increased with increase in feeding level, by 27 % from the low to the medium feeding level and by 33 % from medium to high. Similarly, the estimates of CH_4 emissions expressed per unit of LW increased with increasing feeding levels, by 24% between low and medium feeding levels and by 28% between medium and high feeding levels. These increases were significant ($P < 0.01$), but less than a proportional increase with DMI. Hence, the estimated CH_4 yield per unit of feed intake decreased, by 19 % from the low to the medium feeding level and by 4 % from medium to high (Table 2). Decreasing CH_4 yields at increasing feeding levels were already reported by Blaxter and Clapperton (1965), and have been attributed to a faster rate of passage of feed through the alimentary tract (Benchaar et al., 2001; Pinares-Patiño et al., 2003).

The CH_4 emissions per feed intake are unusually low, compared to the mean for ryegrass-fed cattle in NZ, of 19.1 (±3.70) g CH_4 (kg DMI)$^{-1}$ (Hammond et al., 2009). The observed CH_4 yields, of 4.6, 3.7 and 3.6 % of gross energy intake (GEI), are closer to the IPCC default value for concentrate-fed cattle, 3.0 %, than to the default value for grazing cattle, 6.5 % (IPCC, 2006, p. 10-30). This is likely to be due to the baleage used in this study, in contrast to fresh grass being the usual cattle diet in New Zealand. It is well established (McDonald et al., 1991; Huhtanen and Jaakkola, 1993; González et al., 2007) that ensiling reduces the ruminal degradability of dry matter. A computer simulation by Benchaar et al. (2001) took this effect into account, and also that CH_4 production decreases as pH and acetate/propionate ratio decrease. It predicted that CH_4 emission from feeding lucerne silage would be lower than that from hay (3.7 vs. 5.4 % of GEI). In light of this result, the observed CH_4 yields appear plausible. Yet, a deeper discussion of this finding is beyond the scope of this study.

5.3 Emission rates at the herd scale

For any of the herd-scale techniques, the run-to-run variations of the obtained CH_4 emission rate, Q_c, were considerable. This was the compounded effect of several sources of variability: true emission rate changes in response to the animals' digestion processes, variability of source locations relative to the instruments as the animals moved around, influence of variations in wind speed and direction on the effective footprint of the various techniques, influence of wind speed and direction on the magnitude of the concentration differences to be resolved, and random instrument error (precision). Data availability also differed between techniques. This was partly due to scheduled calibration checks and occasional malfunctions, e.g. dew on optical components, failure of electronic components (resolved by replacement). In addition, wind direction affected availability of the different techniques in different ways. The techniques involving the vertical profile mast (mass-budget and BLS-profile) required the mast to be downwind of at least a few steers, so gave meaningful emission rates only for directions between 210 and 330 °. The techniques involving the two FTIR instruments required one of them to be up- and the other downwind, so data were accepted only if wind direction was within ±50 ° of either W or E. By contrast, the four-path laser system could be used for all wind directions. Periods of low wind speed were excluded for all techniques, when friction velocity was less than 0.1 m s^{-1}.

Given the different operational constraints for each technique, and the overall goal to assess the suitability of each to detect a change between weekly emission rates, the results were first compared on the basis of weekly diurnal courses. To construct these, for each week and technique the 20-min emission rates were sorted by time of day, into 1-h wide bins, and then bin-averaged. The results are discussed in the following subsections.

5.3.1 Diurnal pattern of emissions

Despite obvious discrepancies between techniques, a few features of the emission pattern appear robust (Fig. 7). From about 10:00 h, when the cattle entered their enclosures, Q_c increased steeply until it reached a maximum typically around 13:00 h. In Weeks 1 and 2, Q_c began declining after that, according to all techniques, while in Week 3 the techniques disagreed as to whether Q_c further increased or decreased until 18:00 h. This pattern suggests that the maximum CH_4 emissions typically occurred within 2 h of the time of maximum feeding activity. Feeding always started soon after 10:00 h and in Weeks 1 and 2 was practically finished by noon, while it was stretched out longer in Week 3, when food amounts on offer exceeded the animals' requirements. Similar phase relationships between feeding time and maximum-emission time were observed for feedlot cattle (Loh et al., 2008; Gao et al., 2011) and sheep in test chambers (Lassey et al., 2011). From late afternoon throughout the night, Q_c generally decreased, reaching the lowest levels from about 7:00 to 9:00 h, before the new day's feed ration was offered.

With all herd-scale techniques, Q_c from 10:00 to about 22:00 h (±3 h) was usually larger than the daily average obtained from the SF_6 tracer-ratio technique, and during the other half of the diurnal cycle, Q_c was smaller than the average. This reflected that most of the feeding and ruminating occurred during the daylight hours. Similar activity patterns are common for free-ranging animals.

5.3.2 Profile-based techniques

The mass-budget and BLS technique that used the vertical [CH_4] profile from the closed-path analyser detected virtually the same temporal pattern of emission rates (Fig. 7). On a run-to-run basis, the two techniques agreed typically within 10 %, as was found in other experiments (Laubach and Kelliher, 2005a; Gao et al., 2009; Laubach, 2010).

From one week to the next, the daytime observations (10:00 to 18:00 h) clearly showed increasing Q_c. For the night-time hours, this cannot be stated. On many days the wind direction turned from W in the afternoon, via N in the evening, to NE at night, and then wind speed usually dropped, with friction velocity falling below the acceptance threshold. Since the profile-based techniques relied on westerly wind directions, night-time data availability was poor, and the available data suffered from low replication rates. This is particularly evident in Week 1 (Fig. 7, left panel), where lack of points for some hours, and a lack of error bars for others, indicated that none or only one run per bin, respectively, was available.

Consistently for all three weeks, and almost all times of day, these techniques gave higher Q_c than the other techniques. The likely cause for this is that for most of the time, the animals were not spread evenly across the enclosures. Rather, they preferred to stay near the W fence line. Consequently, for the wind directions most frequent and best-suited for the profile-based techniques, the actual animal density in the effective source area tended to be larger than the nominal mean animal density across the enclosures, which was used for converting emission rates per area to emission rates per animal. Hence, the latter were frequently overestimated. This point is further elaborated in Section 5.5.

5.3.3 BLS with open-path instruments

During the nights of Week 1, the laser system showed the highest data availability of all herd-scale techniques, while no data were available from the FTIR either due to unsuitable wind direction or, during one night, failure of the instrument W of the cattle. During day-time in Week 1, and throughout Weeks 2 and 3, there was generally reasonable agreement in the temporal pattern of Q_c retrieved by BLS from the FTIR and from the laser system. The laser system gave larger variability throughout, indicated both by the error bars in Fig. 7 and the variations from hour to hour. This may appear counter-intuitive, given that the laser system consisted of four paths almost completely surrounding the emission sources, so it should have provided the most representative coverage of the emissions plume for any wind direction. However, the more erratic behaviour of Q_c from the laser system can be explained by its poorer measurement precision.

The BLS results from both open-path systems showed an increase of Q_c from one week to the next. Each week, the hourly averages from the laser system were spread roughly from 0.3 times to 1.7 times the average Q_c from the SF_6 tracer-ratio technique. The corresponding FTIR data spanned roughly between night-time minima (when available) of 0.5 times Q_c and day-time maxima of 1.5 times Q_c from the SF_6 technique.

5.3.4 External tracer-ratio technique

During Week 1, Q_c from the N_2O tracer-ratio technique agreed closely with that from BLS using the same [CH_4] input data from the FTIR (Fig. 7). During Week 2, the N_2O technique gave systematically lower Q_c than BLS, and for many hourly bins the lowest of all herd-scale techniques. The same is true at day-time in Week 3, but not at night. In effect, this technique gave the smallest variations with time of day, tracking the average Q_c from the SF_6 technique more closely than the other herd-scale techniques. This can be explained by the fact that the tracer ratio is independent of the flow field parameters, hence these parameters do not contribute to its error. The sampling errors of the external tracer-ratio technique are those of the mole fractions and the mean N_2O release rate, while for BLS they are those of the mole fractions and a number of wind and turbulence parameters.

5.4 Weekly mean emission rates

To obtain mean CH_4 emission rates for each feeding level, with each technique, the mean diurnal courses were averaged. This gave more representative estimates than simply averaging all available runs, which would have weighted day-time more strongly than night-time (because of the more frequent occurrence of unsuitable calm periods at night). In some instances, especially in Week 1, some night-time hours were not covered by the data, which made some residual bias towards day-time inevitable. Random errors of the weekly means were obtained by propagating the standard errors of the mean for the hourly bins (root-mean-squares estimate). Fig. 8 displays the results, discussed in the following two subsections.

5.4.1 Comparison of absolute mean emission rates

For all three weeks, the techniques using vertical profile data gave the largest mean emission rates. In Week 1, these were 68 and 56 % higher than Q_c from the SF_6 tracer-ratio technique, for mass-budget and BLS, respectively. In Weeks 2 and 3, they exceeded the SF_6 technique consistently by 35 (±2) %. As noted in 5.3.2, the likely main cause for these biases was the systematically uneven animal distribution, resulting in a discrepancy between the actual animal density (in the effective source area of these techniques) and the nominal mean animal density. Another contributing factor was probably the low data yield at night, which could have led to potentially erratic results for some night-time hours. In Week 1, when several night-time hours had no data coverage at all, that would also have led to bias in the diurnal average.

The BLS technique with the four-path laser gave weekly mean Q_c that were 18 % lower than from the SF_6 technique in Week 1, and 8 and 6 % higher (not significantly different) in Weeks 2 and 3, respectively. The low average in Week 1 appears to be caused mostly by low hourly values between 13:00 and 15:00, which do not fit with the diurnal patterns observed in the other weeks and by the other techniques (Fig. 7). Some of the contributing runs with low Q_c had unstable stratification and SE to S winds; it is possible that the N laser path, at only 1.07 m height, was too close to the ground to accurately sample the emissions plume in convective conditions.

The BLS technique with FTIR data exceeded Q_c from the SF_6 technique by 25 and 21 % in Weeks 1 and 2, and agreed within < 1 % (no significant difference) in Week 3. The N_2O tracer-ratio technique exceeded Q_c from the SF_6 technique by 18 % in Week 1, by 3 % (not significant) in Week 2, and fell short of it by 10 % in Week 3 (different at the 95 % confidence level). For both techniques, the overestimate in Week 1 is explained by the lack of night-time data, causing the weekly mean to over-represent the times of feeding activity. For the BLS technique in Week 2, there is no obvious cause for an overestimate. Valid FTIR data were obtained for either W or E winds; the fraction of W winds was 90, 80 and 74 % for Week 1, 2 and 3, respectively, so any effects related to wind direction are unlikely to explain differences between weeks in the BLS technique's performance. For the N_2O tracer-ratio technique in Week 3, it can be seen in Fig. 7 that the day-time emission rates were substantially lower than those recorded by the other techniques. A possible cause for low emission rate estimates is an underestimate of the N_2O release rate, obtained from weighing of the canisters and using the time and temperature dependence determined by Bai (2010). However, the release rates during Week 3 showed very consistent diurnal courses. It thus remains unclear whether the N_2O tracer-ratio technique underestimated the day-time emissions for this week. If it did, that would have caused the weekly average to be an underestimate.

With the exceptions as discussed, it appears that all techniques using open-path [CH_4] measurements delivered weekly mean Q_c that agreed with the enteric tracer-ratio technique within 10 %, which is the commonly assumed magnitude of uncertainty for micrometeorological flux measurement techniques. It should be noted that the herd-scale techniques include CH_4 emissions from the rectum, while the SF_6 tracer-ratio technique does not. Comparisons of the SF_6 technique to animal-chamber measurements by McGinn et al. (2006) and Grainger et al. (2007) indicated lower emission estimates for the SF_6 technique of 4 % and 6 %, respectively, which could in part be attributed to rectal emissions missed by this technique. Accounting for a small underestimate by the SF_6 technique would not change the finding that, for weekly averages, the three open-path techniques agreed well with it. For the two vertical-profile techniques, the differences to the SF_6 technique would be somewhat reduced.

5.4.2 Suitability to resolve a change in mean emission rate

According to the SF_6 tracer-ratio technique, the mean CH_4 emission rate increased by 27 % from Week 1 to 2, and by 33 % from Week 2 to 3. The mass-budget technique failed to detect the first change, but identified an increase of the right magnitude (34 %) for the second. The BLS technique using vertical profile data recorded CH_4 emission increases for both feed level changes, of 10 % and 34 % respectively, but the change from Week 1 to 2 was not significant. For both these techniques, the failure to detect the first step change must be attributed to sparse data coverage and large variability during night-time hours, since Fig. 7 shows that the day-time emission rates increased for both techniques.

The other techniques (N_2O tracer-ratio and BLS with FTIR or four-path laser) detected both changes in weekly emission rates at > 99 % confidence levels. The N_2O tracer-ratio technique recorded the lowest week-to-week increases of these techniques, of 11 and 16 %, respectively, which were just under half of the increases shown by the SF_6 technique. For the first step change, this can be explained by the overestimate in Week 1 due to a lack of night-time data. For the second step change, this is computationally caused by low day-time emission rates in Week 3, yet the ultimate cause for these is unclear.

Since the 95 % confidence intervals are about twice and 99 % confidence intervals roughly 3 times as large as the standard errors in Fig. 8, one may infer that (in all instances where data availability was sufficient) all techniques would probably detect changes of order 20 % with 99 % confidence, and changes of order 10 % with 95 % confidence. Such inferences should of course be tested with separate experiments.

5.5 Sensitivity of emission estimates to animal distribution

All herd-scale techniques except for the N_2O tracer-ratio technique derived the CH_4 emission rate on a per-area basis, and for that required specification of the shape and extent of the emissions' source area (as determined by the fence lines). The per-area emissions were then converted into per-animal emission rates, with the same conversion factor for all techniques (61.8 m^2 $animal^{-1}$). However, as noted before, for most of the time the steers did not spread evenly across the fenced area. A sensitivity study was undertaken to assess how the uneven spread affected the emission rate estimates from the different techniques, by defining a "cattle-preference" area that excluded the rarely-visited NE and SE corners of the enclosure (Fig. 9).

One effect of this changed area specification is common to all techniques: it reduces the conversion factor by 16.2 %, to 51.8 m^2 $animal^{-1}$. Further effects differ between the techniques. For the mass-budget technique, the source area contact distance upwind of the mast, traversed by the air flow, is reduced, but only for the marginally acceptable wind directions more than ±40 ° off W, not for the wind directions around W. For the BLS technique, the "touchdown" statistics (where the backwards-tracked air parcels are in contact with the ground) remain unaltered, but the classification which touchdowns contribute to the downwind concentration elevation changes, which leads to altered three-dimensional concentration fields (normalised by Q_c, which is assumed homogeneous within the source area). The net effect of that is expected to differ for different arrays of sensor locations (vertical profile, two-path system, and four-path system).

The results of the sensitivity tests are evaluated by taking the ratio of the emission rate with the "cattle-preference" area prescribed as the source to the emission rate with the fenced enclosure prescribed as the source. In Fig. 10, this ratio is displayed against wind direction. Distinct relationships are observed, for each technique. They display some scatter that stems from the variability of the turbulent flow parameters, mainly stability and the standard deviation of the crosswind fluctuations. Fig. 10 also implicitly provides an overview how the accepted runs, for each technique, were distributed with wind direction.

The relationships for the mass-budget and the BLS technique using the same vertical [CH_4] profile are virtually identical. This is reassuring because it means the way in which crosswind fluctuations are accounted for in the mass-budget approach of Laubach and Kelliher (2004) is in agreement with the Lagrangian simulation statistics. For these two techniques, the reduced conversion factor determines the result in the sector from 230 to 310 °, while outside this sector there is a steep rise in the ratio with increasing angular distance from 270 °. As W winds dominated throughout the campaign, the net effect of prescribing the "cattle-preference" area on the weekly mean Q_c would be a reduction by 10 to 16 % in each week. The reduced Q_c would be in better agreement with the two tracer-ratio techniques. The high sensitivity to source area choice is the biggest disadvantage of the vertical-profile techniques. It could be reduced by increasing the distance between sources and sensors, as recommended by Flesch et al. (2005), but at the cost of further narrowing the range of acceptable wind directions. Here, the sensitivity to source area choice, especially for the marginal wind directions, may go some way to explain why the step change from Week 1 to 2 was not detected by the vertical-profile techniques.

For the two-path FTIR system, the changed source area prescription leads to an increase of Q_c for westerly winds, by 10 to 20 %, and to a decrease for easterly winds, by 5 to 10 % (Fig. 10). The result is not symmetrical because of the different distances between FTIR path and nearest enclosure fence in W and E, respectively. The increase for W directions can be qualitatively understood as follows. The same downwind line-integrated [CH_4] as before is now interpreted to be caused by an emitting area that is (in its N and S parts) farther away from the receptor path than with the original source area prescription. The longer distance would cause enhanced dilution by turbulent dispersion in all dimensions. To counter that dilution effect, the model must assign an increased emission rate to the source area, in higher proportion than that necessary to compensate for its reduced size. For E wind directions, the situation is different: the distance between the W boundary of the source area and the then-downwind W receptor path is unchanged. The source area extent is reduced in the corners farthest away from the receptor path, which had the smallest touchdown density and thus made the smallest relative contribution to the [CH_4] signal. Consequently, the BLS model computes an emission rate for the reduced area that is increased less than proportionally, compared to the result for the total fenced area, and a smaller emission rate per animal results. Because W winds were far more frequent than E winds (Fig. 10), the effect of the changed source area prescription on the weekly mean Q_c

from the FTIR would be an increase, of order 10 %. This would decrease the differences to the vertical-profile techniques, but would on the other hand increase the differences to the two tracer-ratio techniques.

The pattern for the four-path laser-system is quite different to that for the two-path FTIR system (Fig. 10). For most wind directions, the change caused by the re-definition of the source area is within ±10 %. Systematic decreases larger than that occur around 120, 225 and 320 °, which are “diagonal” directions towards corners poorly covered by downwind receptor paths (see Fig. 1); longer paths reaching past the corners would probably have reduced the extent of these decreases. Overall, it appears that the four-path setup is the least sensitive to the exact source area specification, because the touchdown coverage achieved with multiple paths is more evenly distributed than for setups with a single downwind path or point (mast). Fig. 10 suggests that the effect of the re-defined source area on the weekly mean Q_c would have been within ±5 %, so despite the poorer precision of the laser system, compared to the other CH_4 instruments, the average results were robust.

6. Conclusions

Weekly-averaged CH_4 emission rates from a herd of steers fed with pasture baleage correlated strongly with dry-matter intake, yet less than proportionally. According to the enteric tracer-ratio technique, the increases in emission rate from one week to the next were 27 and 33 %, respectively. Comparing the five herd-scale techniques against this animal-scale technique and against each other yielded the following results and insights:

- All techniques were able to detect the increase from Week 2 to 3 with > 99 % confidence. The open-path-based techniques and the animal-scale technique also detected the increase from Week 1 to 2 with > 99 % confidence.
- The techniques based on vertical [CH_4] profiles were carried out with the most accurate and well-calibrated CH_4 instrument, but they were prone to the lowest data yield, due to wind direction restrictions, and were the most sensitive to inhomogeneous spatial distribution of sources.

- The techniques based on path-averaged [CH_4] measurements generally gave accurate weekly emission rates (within 10 % of the enteric tracer-ratio technique).
- The external tracer-ratio technique, which is inherently insensitive to uneven source distribution, provided emission rates with the smallest run-to-run variability of all techniques. This advantage in precision came at the cost of considerable extra effort to provide suitable tracer release at the exact CH_4 source locations. However, on a week-to-week basis, this technique possibly underestimated the changes in mean emission rate.
- With the BLS technique, four measurement paths offer significant advantages over two, not only in providing higher data yield (by including all wind directions), but also in being less sensitive to uneven source distribution. This was demonstrated by the laser system delivering unbiased weekly emission rates, despite the poorer accuracy of its individual mixing-ratio measurements.

These findings suggest as the ideal herd-scale technique one that combines the strengths of the accurate closed-path analyser with the strengths of a path-averaging approach. This could be done either by using horizontally-aligned arrays of many intakes, drawing air simultaneously to a closed-path analyser (e.g. perforated intake tubes), or by using high-quality open-path instruments, like the FTIR, in conjunction with regular cross-checks against such an analyser.

Of interest from the perspectives of animal nutrition and greenhouse gas emissions mitigation is that this experiment, using grass baleage as feed, recorded far lower CH_4 yields per feed intake than ever found with fresh grass. It should be followed up in further studies which properties of the baleage effected this result.

Acknowledgements

The experiment and the involvement of the NZ-based authors were funded by New Zealand's Foundation of Research, Science and Technology (FRST) until 2011, and by Core Funding for Crown Research Institutes from the Ministry of Business, Innovation and Employment’s Science and Innovation Group since. The participation of the University of Wollongong was funded by ARC Linkage Grant LP0561000. E. A.

Cárdenas R. received a fellowship from the Livestock Emissions Abatement Research Network (LEARN) of NZ’s Ministry for Agriculture and Forestry. The experiment would not have been possible without the logistical backing of Steve Lees (Aorangi Farm) and his staff. We thank Dan Robinson for drafting the animals and weighing and distributing their feed supply, Edgar Sandoval for help with the animal handling, and Sarah McLean and Grant Taylor for laboratory analyses (all AgResearch). Tony McSeveny and Peter Berben (Landcare Research) were instrumental in setting up the scientific equipment. We thank Dr Frank Kelliher for the initial idea of this experiment and valuable advice throughout the planning stages.

Appendix: Temperature dependence of the open-path methane laser

The open-path CH_4 laser system (Boreal Laser, 2005) reports its measurement as a mole fraction χ (ppm), despite the fact that the absorption along the measurement path depends primarily on the absolute density of CH_4 molecules on the path, ρ_c (mol m^{-3} or kg m^{-3}). The reported mole fraction is only correct at an assumed reference temperature, T_{ref}, and pressure, p_{ref}. In general, though, actual temperature, T, and pressure, p, along the path will differ from these reference values, in which case the CH_4 mole fraction requires correction. There are three mechanisms by which T and p affect the mole fraction.

The first of these mechanisms is the universal gas law. If this was the only one, then the correct mole fraction, χ_{corr}, could be obtained from the reported mole fraction, χ_{meas}, as:

$$\chi_{corr} = \chi_{meas}\,(T\,p_{ref})/(T_{ref}\,p) \qquad \text{(A1)}$$

with temperatures in K. The relative sensitivity of χ to temperature change (for $p = p_{ref}$) would be obtained as $\chi^{-1}\,\partial\chi/\partial T = T_{ref}^{-1} = 3.37 \cdot 10^{-3}$ K^{-1}, at $T = T_{ref} = 296$ K (the choice of value is explained below). For example, a deviation of T from T_{ref} by 3 K would produce 1 % relative error in χ, equivalent to 17 ppb absolute error at the global background mole fraction. A similar error would result from a difference of 1 kPa between p and p_{ref}, assuming the standard value $p_{ref} = 101.3$ kPa. When determining emission rates, mole fraction differences between two measurement locations are crucial input variables. Assuming that temperature and pressure at the two locations were equal, the mole fraction difference would be subject to the same relative error as the mole fraction itself, and so would be the computed emission rate.

The second mechanism is the dependence of the spectral intensity of the absorption line, S, on temperature. In first-order approximation, this can be written as:

$$S(T) = S(T_{ref}) \exp(-b\, E_0/T) \,/\, \exp(-b\, E_0/T_{ref}) \tag{A2}$$

where E_0 is the energy of the lower state of the transition (in cm^{-1}), $b = 1.438775$ K cm is a collection of fundamental constants (Planck constant times speed of light in vacuum divided by Boltzmann constant), sometimes referred to as the "second radiation constant", and T_{ref} is a reference temperature, which is set to 296 K in the spectroscopic database HITRAN (Rothman et al. 1998, 2005). The arguments of the exponential function in (A2) quantify the probability with which the lower state is occupied for a given temperature. In (A2), the effects of the partition function and of stimulated emission are neglected; the full equation can be found e.g. in Rothman et al. (1998, their Eq. A11). Differentiating (A2) and normalising by S results in:

$$S^{-1}\, dS/dT = b\, E_0/T^2 \tag{A3}$$

The absorption line feature used by the GasFinder is the R3 triplet in the $2\nu_3$ band, centred at the wavenumber 6046.953 cm^{-1} (J. Tulip, Boreal Laser, pers. comm., 2003). The HITRAN database (Rothman et al., 2005) gives E_0 for each line of the triplet with 6 digits precision; each E_0 can be rounded to 62.88 cm^{-1}. Using this value to evaluate (A3) at $T = T_{ref}$ gives $S^{-1}\, dS/dT = 1.03 \cdot 10^{-3}\, K^{-1}$. Since observed absorbance is proportional to S, this relative temperature sensitivity of spectral intensity also applies to the reported mole fraction. It is about 0.3 of the gas-law temperature sensitivity.

The third mechanism is band-broadening of the absorption line. Some of this is caused by collisions of the absorbing molecules with other molecules which subtly alter the energy of the transition between the quantum states; this increases with increasing pressure (increasing the probability for collisions). There is also band-broadening due to the Doppler effect; this increases with increasing temperature (Hollas, 2004). While the HITRAN database provides parameters to estimate broadening effects, these do not include the effects of potentially highly variable water vapour concentration (Tuzson et al., 2010). Also, Frankenberg et al. (2008) point out that the catalogued broadening parameters are by no means certain, and for multiplets in the $2\nu_3$ band of CH_4 almost impossible to model. Further, the net effect of band-broadening on the line-shape retrieval algorithm would have to be modelled or experimentally determined, which is beyond the scope of this study.

To complicate matters further, instrument-specific parameters also influence the temperature and pressure sensitivity of the GasFinder (J. Terry, Boreal Laser, pers. comm., 2012). According to correction curves determined by the manufacturer, the net sensitivity of χ to pressure in the range 97 to 105 kPa is typically within ±0.3 % kPa^{-1}. Over the pressure range of the present experiment (100.0 to 102.7 kPa), this sensitivity has only minor effect, compared to the temperature dependence from all mechanisms combined. For the GasFinder system used here, the total temperature sensitivity was found about 2.5 times that from the gas law alone. The interaction of spectroscopic effects with instrument parameters is therefore important, however not fully predictable. Because of that, the temperature sensitivities of any two GasFinder systems will probably differ, and individual calibration is recommended.

References

Bai, M., 2010. Methane emissions from livestock measured by novel spectroscopic techniques. PhD thesis, University of Wollongong, Australia, 303 pp.

Benchaar, C., Pomar, C., Chiquette, J., 2001. Evaluation of dietary strategies to reduce methane production in ruminants: A modelling approach. Can. J. Anim. Sci., 81: 563-574.

Blaxter, K.L., Clapperton, J.L., 1965. Prediction of the amount of methane produced by ruminants. British J. of Nutrition, 19: 511-22.

Boreal Laser, 2005. GasFinderMC Operation Manual. Boreal Laser Inc., Spruce Grove, Alberta, Canada, 79 pp.

CSIRO, 2007. Nutrient Requirements of Domesticated Ruminants. CSIRO Publishing, Collingwood, Victoria, Australia, 270 pp.

Flesch, T. K., Wilson, J. D., Yee, E., 1995. Backward-time Lagrangian stochastic dispersion models, and their application to estimate gaseous emissions. J. Appl. Meteorol., 34: 1320-1332.

Flesch, T. K., Wilson, J. D., Harper, L. A., Crenna, B. P., and Sharpe, R. R., 2004. Deducing ground-air emissions from observed trace gas concentrations: a field trial. J. Appl. Meteorol., 43: 487-502.

Flesch, T. K., Wilson, J. D., Harper, L. A., and Crenna, B. P., 2005. Estimating gas emissions from a farm with an inverse-dispersion technique. Atmos. Environ., 39: 4863-4874.

Frankenberg, C., Warneke, T., Butz, A., Aben, I., Hase, F., Spietz, P., and Brown, L. R., 2008. Pressure broadening in the $2\nu_3$ band of methane and its implication on atmospheric retrievals. Atmos. Chem. Phys., 8: 5061-5075.

Gao, Z., Desjardins, R. L., and Flesch, T. K., 2009. Comparison of a simplified micrometeorological mass difference technique and an inverse dispersion technique for estimating methane emissions from small area sources. Agric. For. Meteorol., 149: 891-898.

Gao, Z., Yuan, H., Ma, W., Liu, X., and Desjardins, R. L., 2011. Methane emissions from a dairy feedlot during the fall and winter seasons in Northern China. Environmental Pollution, 159: 1183-1189.

González, J., Faría-Mármol, J., Rodríguez, C.A., Martínez, A., 2007. Effects of ensiling on ruminal degradability and intestinal digestibility of Italian rye-grass. Anim. Feed Sci. Technol., 136: 38-50.

Grainger, C., Clarke, T., McGinn, S. M., Auldist, M. J., Beauchemin, K. A., Hannah, M. C., Waghorn, G. C., Clark, H., and Eckard, R. J., 2007. Methane emissions from dairy cows measured using the sulfur hexafluoride (SF_6) tracer and chamber techniques. J. Dairy Sci., 90: 2755-2766.

Griffith, D. W. T., 1996. Synthetic calibration and quantitative analysis of gas-phase FT-IR spectra. Appl. Spectrosc., 50: 59-70.

Griffith, D. W. T., Bryant, G. R., Hsu, D., and Reisinger, A. R., 2008. Methane emissions from free-ranging cattle: Comparison of tracer and integrated horizontal flux techniques. J. Environ. Qual., 37: 582-591.

Griffith, D. W. T., Deutscher, N. M., Caldow, C. G. R., Kettlewell, G., Riggenbach, M., and Hammer, S., 2012. A Fourier transform infrared trace gas and isotope analyser for atmospheric applications. Atmos. Meas. Tech., 5: 2481-2498.

Hammond, K. J., Muetzel, S., Waghorn, G. C., Pinares-Patiño, C. S., Burke, J. L., and Hoskin, S. O., 2009. The variation in methane emissions from sheep and cattle is not explained by the chemical composition of ryegrass. Proceedings of the New Zealand Society of Animal Production, 69: 174-178.

Harper, L. A., Denmead, O. T., Freney, J. R., and Byers, F. M., 1999. Direct measurements of methane emissions from grazing and feedlot cattle. J. Anim. Sci., 77: 1392-1401.

Harper, L. A., Denmead, O. T., and Flesch, T. K., 2011. Micrometeorological techniques for measurement of enteric greenhouse gas emissions. Anim. Feed Sci. Technol., 166-167: 227-239.

Hollas, J. M., 2004. Modern Spectroscopy, 4th ed. John Wiley & Sons, Chichester, England, 452 pp.

Huhtanen, P., Jaakkola, S., 1993. The effects of forage preservation method and proportion of concentrate on digestion of cell wall carbohydrates and rumen digesta pool size in cattle. Grass Forage Sci., 48: 155-165.

IPCC, 2006. 2006 IPCC Guidelines for National Greenhouse Gas Inventories, Volume 4: Agriculture, Forestry and Other Land Use. Available online at http://www.ipcc-nggip.iges.or.jp/public/2006gl/vol4.html.

Johnson, K., Huyler, M., Westberg, H., Lamb, B., Zimmerman, P., 1994. Measurement of methane emissions from ruminant livestock using a SF_6 tracer technique. Environ. Sci. Technol., 28: 359-362.

Lassey, K. R., 2007. Livestock methane emission: from the individual grazing animal through national inventories to the global methane cycle. Agric. For. Meteorol., 142: 120-132.

Lassey, K. R., Pinares-Patiño, C. S., Martin, R. J., Molano, G., and McMillan, A. M. S., 2011. Enteric methane emission rates determined by the SF_6 tracer technique: Temporal patterns and averaging periods. Anim. Feed Sci. Technol., 166-167: 183-191.

Laubach, J., 2010. Testing of a Lagrangian model of dispersion in the surface layer with cattle methane emissions. Agric. For. Meteorol., 150: 1428-1442.

Laubach, J., and Kelliher, F. M., 2004. Measuring methane emission rates of a dairy cow herd by two micrometeorological techniques. Agric. For. Meteorol., 125: 279-303.

Laubach, J., and Kelliher, F. M., 2005a. Measuring methane emission rates of a dairy cow herd (II): results from a backward-Lagrangian stochastic model. Agric. For. Meteorol., 129: 137-150.

Laubach, J., and Kelliher, F. M., 2005b. Methane emissions from dairy cows: Comparing open-path laser measurements to profile-based techniques. Agric. For. Meteorol., 135: 340-345.

Laubach, J., Kelliher, F. M., Knight, T., Clark, H., Molano, G., and Cavanagh, A., 2008. Methane emissions from beef cattle – a comparison of paddock- and animal-scale measurements. Aust. J. Exp. Agric., 48: 132-137.

Leuning, R., Baker, S. K., Jamie, I. M., Hsu, C. H., Klein, L., Denmead, O. T., and Griffith, D. W. T., 1999. Methane emission from free-ranging sheep: a comparison of two measurement methods. Atmos. Environ., 33: 1357-1365.

Loh, Z., Chen, D., Bai, M., Naylor, T., Griffith, D., Hill, J., Denmead, T., McGinn, S., and Edis, R., 2008. Measurement of greenhouse gas emissions from Australian feedlot beef production using open-path spectroscopy and atmospheric dispersion modelling. Aust. J. Exp. Agric., 48: 244-247.

McDonald, P., Henderson, A.R., Heron, S.J.E., 1991. The Biochemistry of Silage, 2nd ed. Chalcombe Publications, Marlow, Bucks., England, 340 pp.

McGinn, S. M., Beauchemin, K. A., Iwaasa, A. D., and McAllister, T. A., 2006. Assessment of the sulfur hexafluoride (SF_6) tracer technique for measuring enteric methane emissions from cattle. J. Environ. Qual., 35: 1686-1691.

Pinares-Patiño, C.S., Ulyatt, M.J., Lassey, K.R., Barry, T.N., Holmes, C.W., 2003. Rumen function and digestion parameters associated with differences between sheep in methane emissions when fed chaffed lucerne hay. J. Agric. Sci. Camb., 140: 205-214.

Pinares-Patiño, C. S., Waghorn, G. C., Machmüller, A., Vlaming, B., Molano, G., Cavanagh, A. and Clark, H., 2007. Methane emissions and digestive physiology of non-lactating dairy cows fed pasture forage. Can J. Anim. Sci., 87: 601-613.

Rothman, L. S., Rinsland, C. P., Goldman, A., Massie, S. T., Edwards, D. P., Flaud, J.-M., Perrin, A., Camy-Peyret, C., Dana, V., Mandin, J.-Y., Schroeder, J., McCann, A., Gamache, R. R., Wattson, R. B., Yoshino, K., Chance, K. V., Jucks, K. W., Brown, L. R., Nemtchinov, V., and Varanasi, P., 1998. The HITRAN molecular spectroscopic database and HAWKS (HITRAN Atmospheric Workstation): 1996 edition. J. Quant. Spectrosc. Radiat. Transfer, 60: 665-710.

Rothman, L. S., Jacquemart, D., Barbe, A., Benner, D. C., Birk, M., Brown, L. R., Carleer, M. R., Chackerian Jr, C., Chance, K., Coudert, L. H., Dana, V., Devi, V. M., Flaud, J.-M., Gamache, R. R., Goldman, A., Hartmann, J.-M., Jucks, K. W., Maki, A. G., Mandin, J.-Y., Massie, S. T., Orphal, J., Perrin, A., Rinsland, C. P., Smith, M. A. H., Tennyson, J., Tolchenov, R. N., Toth, R. A., Vander Auwera, J., Varanasi, P., and Wagner, G., 2005. The HITRAN 2004 molecular spectroscopic database. J. Quant. Spectrosc. Radiat. Transfer, 96: 139-204.

Smith, T. E. L., Wooster, M. J., Tattaris, M., and Griffith, D. W. T., 2011. Absolute accuracy and sensitivity analysis of OP-FTIR retrievals of CO_2, CH_4 and CO over concentrations representative of “clean air” and “polluted plumes”. Atmos. Meas. Tech., 4: 97-116.

Tuzson, B., Hiller, R. V., Zeyer, K., Eugster, W., Neftel, A., Ammann, C., and Emmenegger, L., 2010. Field intercomparison of two optical analyzers for CH_4 eddy covariance flux measurements. Atmos. Meas. Tech., 3: 1519-1531.

Tables

Table 1 Overview of the techniques used to determine CH_4 emission rates from 61 cattle, and the associated instrumentation for each technique.

Technique	Instrumentation	Institution
Animal scale:		
Enteric tracer-ratio	SF_6 release in rumen, yokes on cattle, GC analysis	AgRes
Herd scale:		
External tracer-ratio	N_2O release canisters on cattle, open-path FTIR	UoW
Mass-budget	Los Gatos with 7 intakes, cup anemometer profile	LCR
BLS from profile	Los Gatos with 7 intakes, cup & sonic anemometer	LCR
BLS from 4 paths	GasFinder MC, cup & sonic anemometer	LCR
BLS from 2 paths	open-path FTIR, cup & sonic anemometer	UoW

AgRes = AgResearch, LCR = Landcare Research, UoW = University of Wollongong

Table 2 The steers' average liveweight, estimated feed on offer, feed intake, and methane emissions (as obtained with the SF_6 tracer-ratio technique) at the three feeding levels. Values in parentheses are standard deviations, unless indicated otherwise [1].

Period Feeding level	Week 1 Low	Week 2 Medium	Week 3 High	P value [4]
Liveweight (kg)	331 (21)	339 (21)	352 (22)	n.d.
Feed (kg DM d^{-1} $animal^{-1}$):				
offered [1]	4.30 (0.09)	6.78 (0.15)	10.32 (0.23)	n.d.
refused (soiled) [2]	0.04	0.06	1.03 (0.33)	n.d.
intake [1]	4.26 (0.10)	6.72 (0.16)	9.29 (0.40)	n.d.
CH_4 emissions:				
g CH_4 d^{-1} $animal^{-1}$	70.8 (13.5)	89.7 (11.1)	119.1 (16.4)	<0.001
g CH_4 d^{-1} (kg LW)$^{-1}$	0.213 (0.036)	0.265 (0.028)	0.338 (0.039)	<0.001
g CH_4 (kg DMI)$^{-1}$	16.6	13.4	12.8	n.d.
Y_m (% of GEI) [3]	4.6	3.7	3.6	n.d.

[1] Feed values per individual animal were calculated by dividing the estimated total for the herd by the number of animals, hence no s.d. is available. The indicated uncertainties are estimated weighing errors for the feed offered, and propagated from weighing error and visual estimation of refused amounts for feed intake.

[2] The amount of soiled feed was estimated by eye as a proportion of feed on offer: < 1 %, < 1 % and 10 % at low, medium and high feeding levels, respectively.

[3] Methane yield: methane energy as percentage of the gross energy intake (GEI).

[4] Probability value for feeding level effect; n.d. = not determined.

Figures

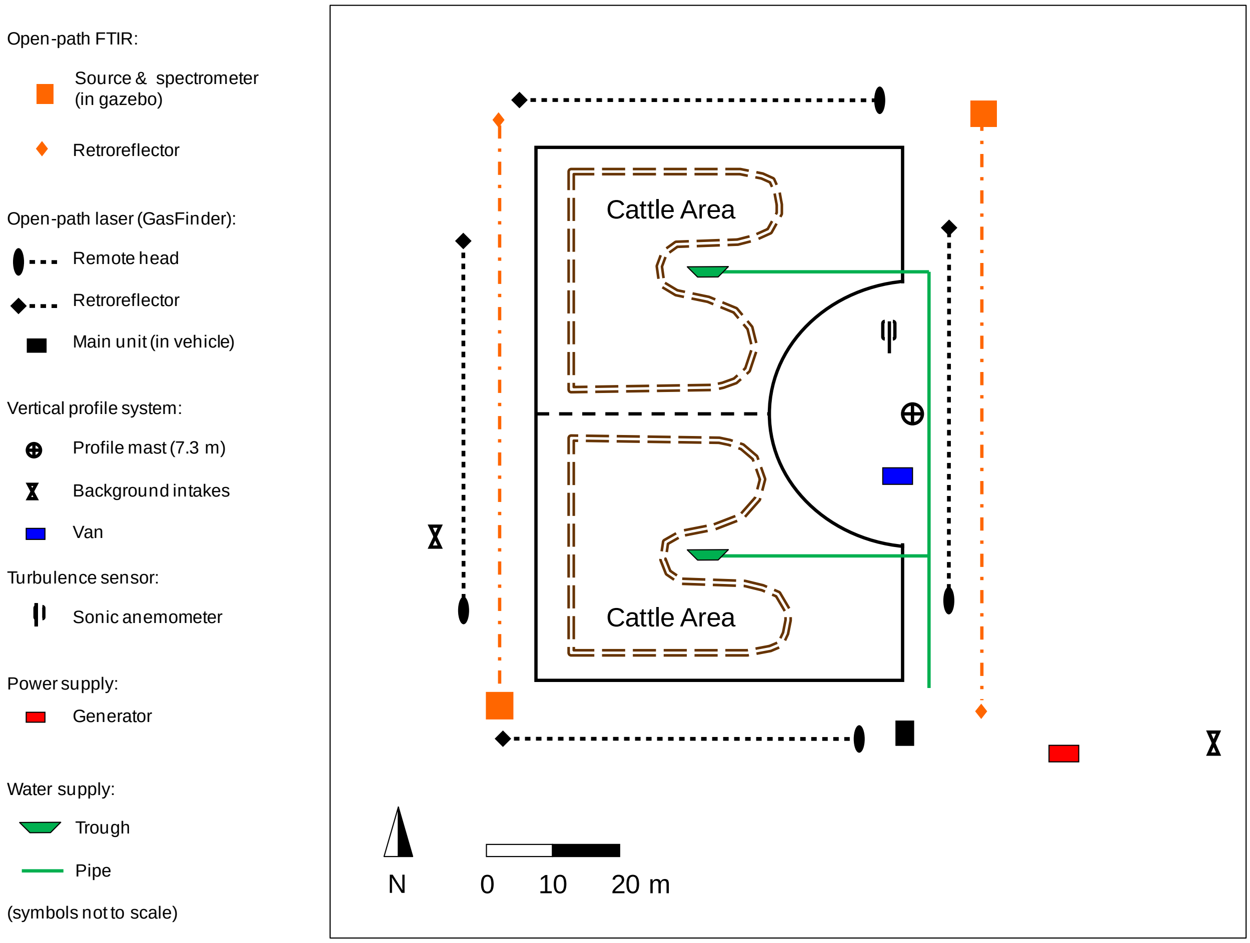

Fig. 1 Schematic of the experimental setup. The cattle area was subdivided into two equal-sized enclosures (dashed line), occupied by 30 and 31 animals, respectively. Every morning, baleage feed was laid out approximately as indicated by the "B"-shaped double-dashed lines.

a)

b)

Fig. 2 The source/detector arrays of the two types of open-path instruments used: a) GasFinder MC infrared laser (Boreal Laser Inc.), b) FTIR spectrometer (University of Wollongong).

Fig. 3 A steer wearing the collection yoke – the white pipe around his neck – for the enteric tracer-ratio (SF_6) technique, as well as the N_2O release canister for the external tracer-ratio technique, in a grey bag attached to the left front of the yoke.

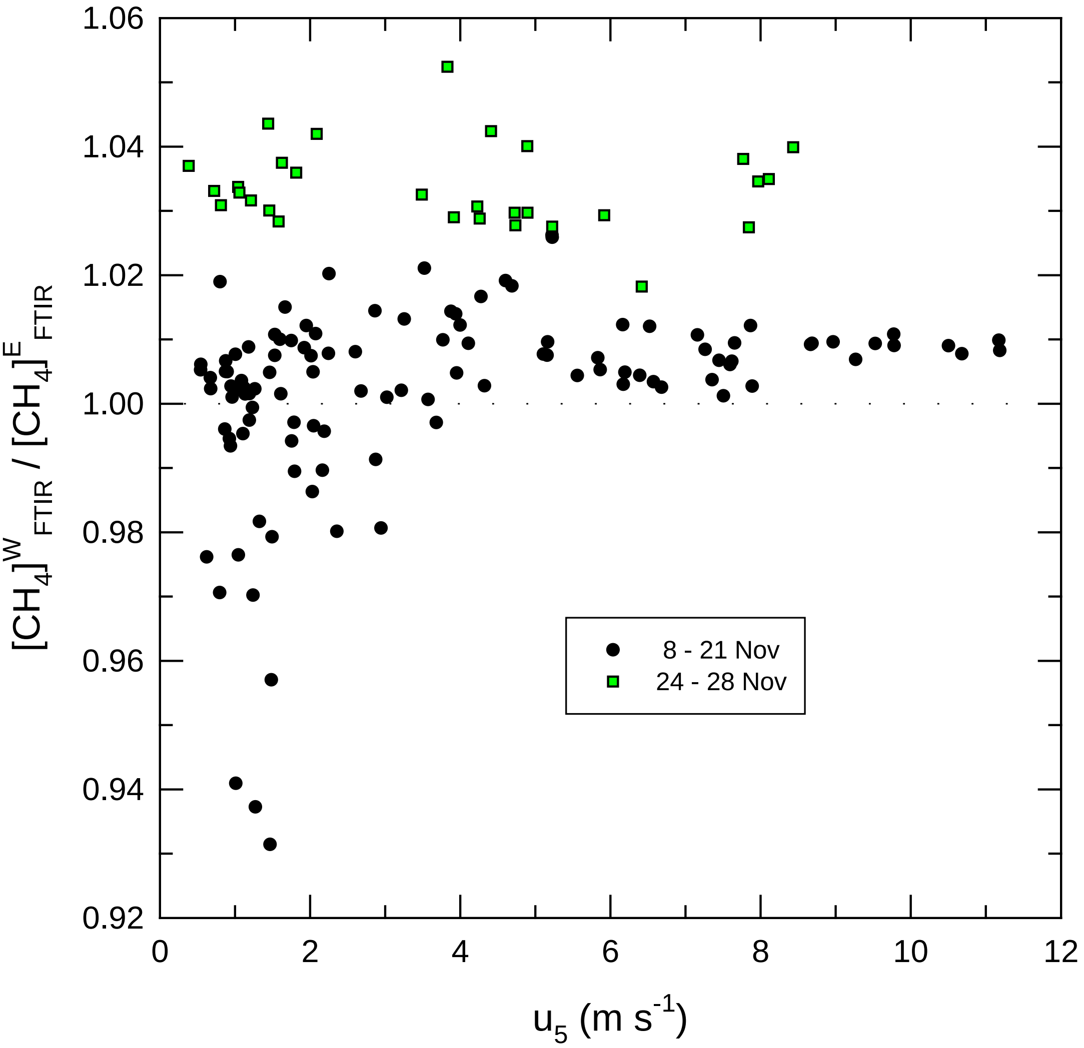

Fig. 4 Ratio of FTIR-measured uncorrected CH_4 mole fractions, from W path to E path, for times of cattle absence, against wind speed at 7.18 m. There were no periods of cattle absence on 22 to 23 Nov. From 22 to 24 Nov, the W FTIR experienced an electronics failure. Rectifying this necessitated a realignment, after which some calibration parameters had changed.

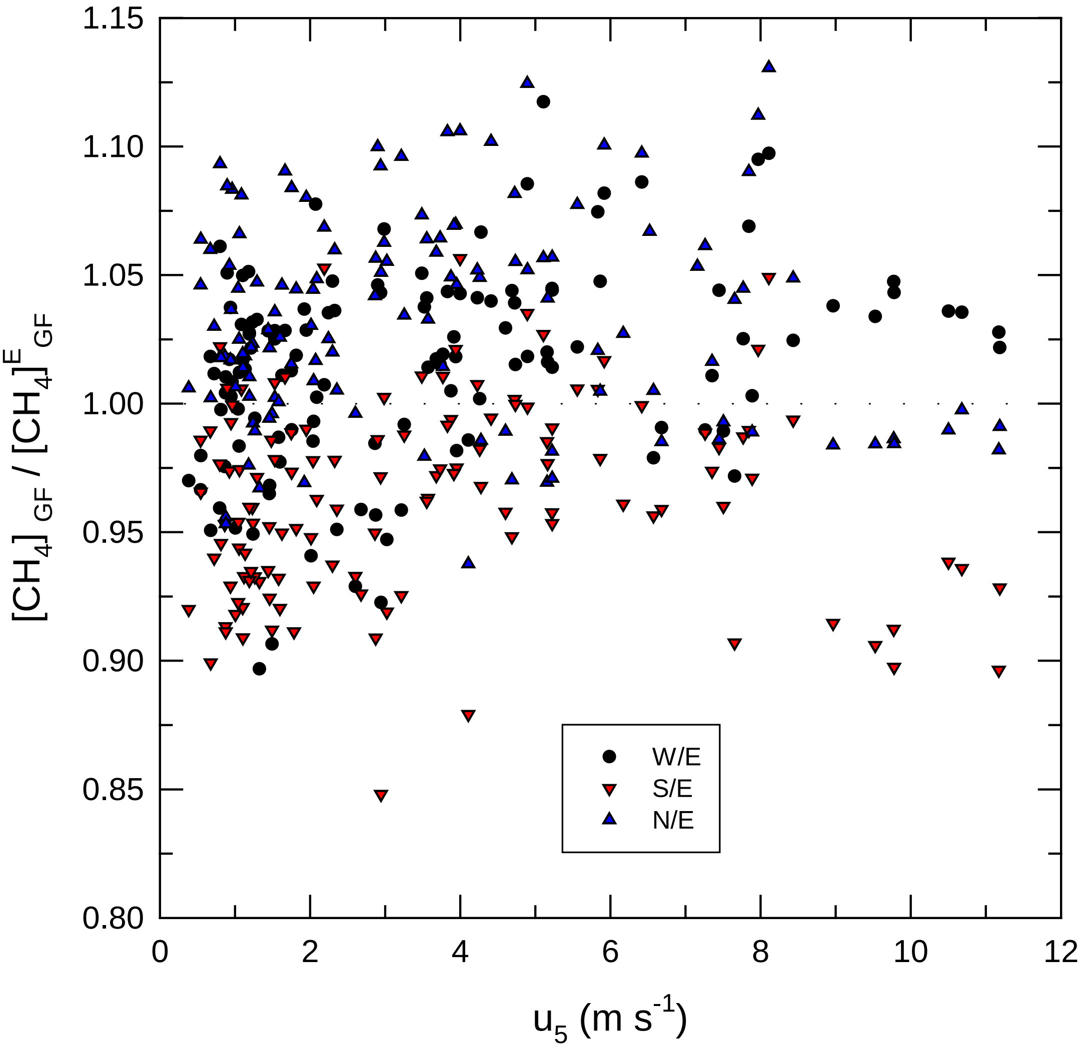

Fig. 5 Ratios of the open-path laser's CH_4 mole fractions, from W, S and N path relative to E path, for times of cattle absence, against wind speed at 7.18 m.

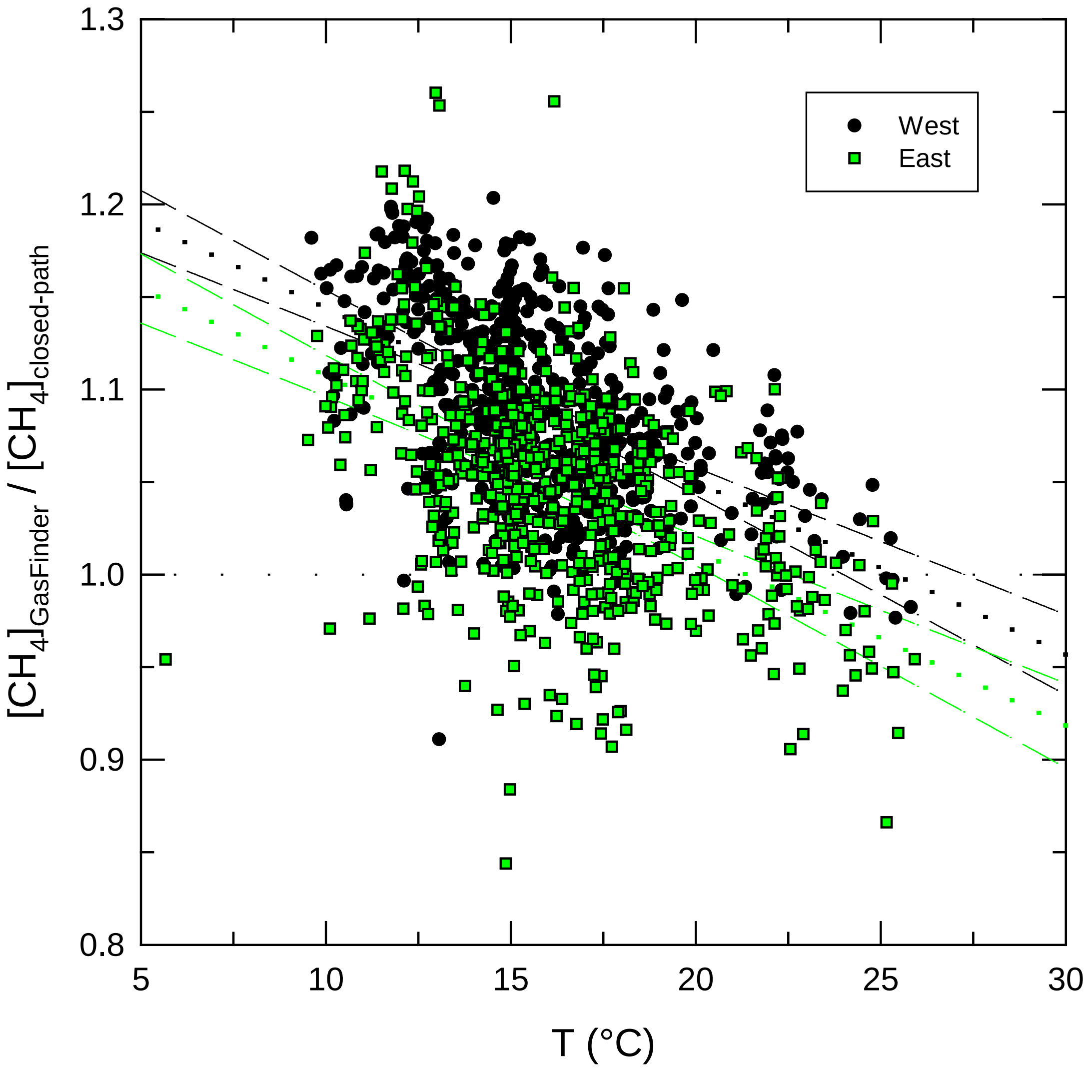

Fig. 6 Ratio of CH_4 mole fractions from open-path laser (GasFinder) and closed-path analyser (Los Gatos) against temperature, for periods with $u_5 > 2$ m s^{-1}. Short-dashed lines: linear regression curves separately for W path (dots, 621 points, $R^2 = 0.30$) and E path (squares, 649 points, $R^2 = 0.26$), long-dashed lines: 99 %-confidence intervals. The regression slope is the same for both, -9.4×10^{-3} K^{-1}.

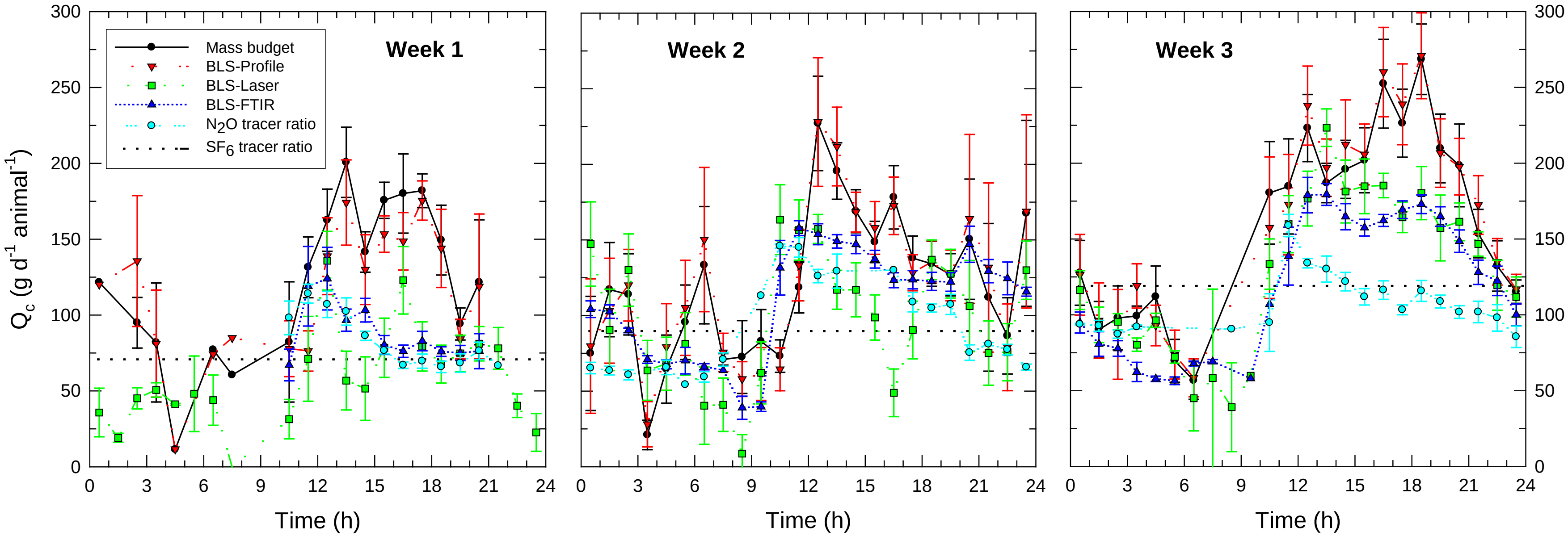

Fig. 7 Mean diurnal courses of CH_4 emission rates obtained with the five herd-scale techniques, with error bars indicating standard error of the mean for each hourly bin. The three panels are for low, medium and high feeding level, from left to right. The weekly mean emission rate from the animal-scale SF_6 technique is indicated as a horizontal dashed line in each panel.

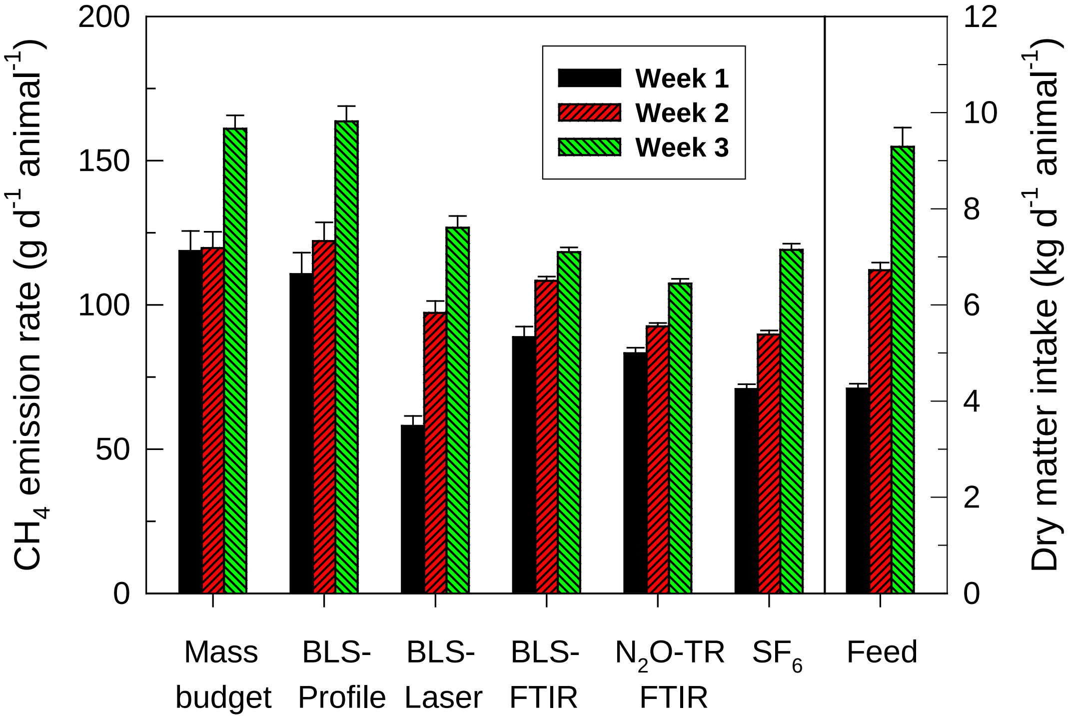

Fig. 8 Mean weekly CH_4 emission rates for each technique, obtained by averaging the mean diurnal courses of Fig. 7. Error bars indicate propagated errors (from the hourly standard errors) for the five herd-scale techniques, and the standard error of the mean from 61 animals for the animal-scale SF_6 technique. The right-most set of columns shows the feed intake, with estimated errors from weighing and visual assessment of refusal.

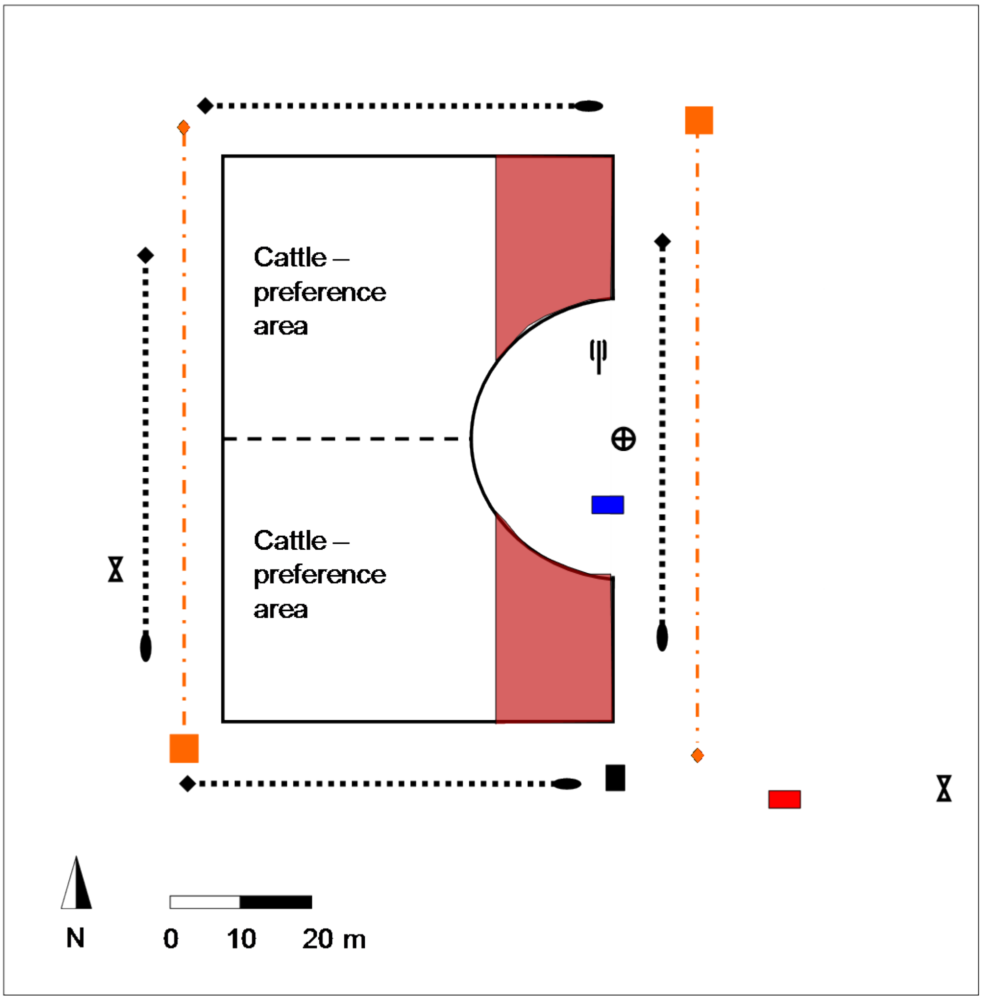

Fig. 9 Schematic of the experimental setup as in Fig. 1, but with the eastern areas that were rarely visited by the cattle indicated in dark colour. These areas were not considered part of the source area when CH_4 emission rates were re-computed for the “cattle-preference area”.

1145

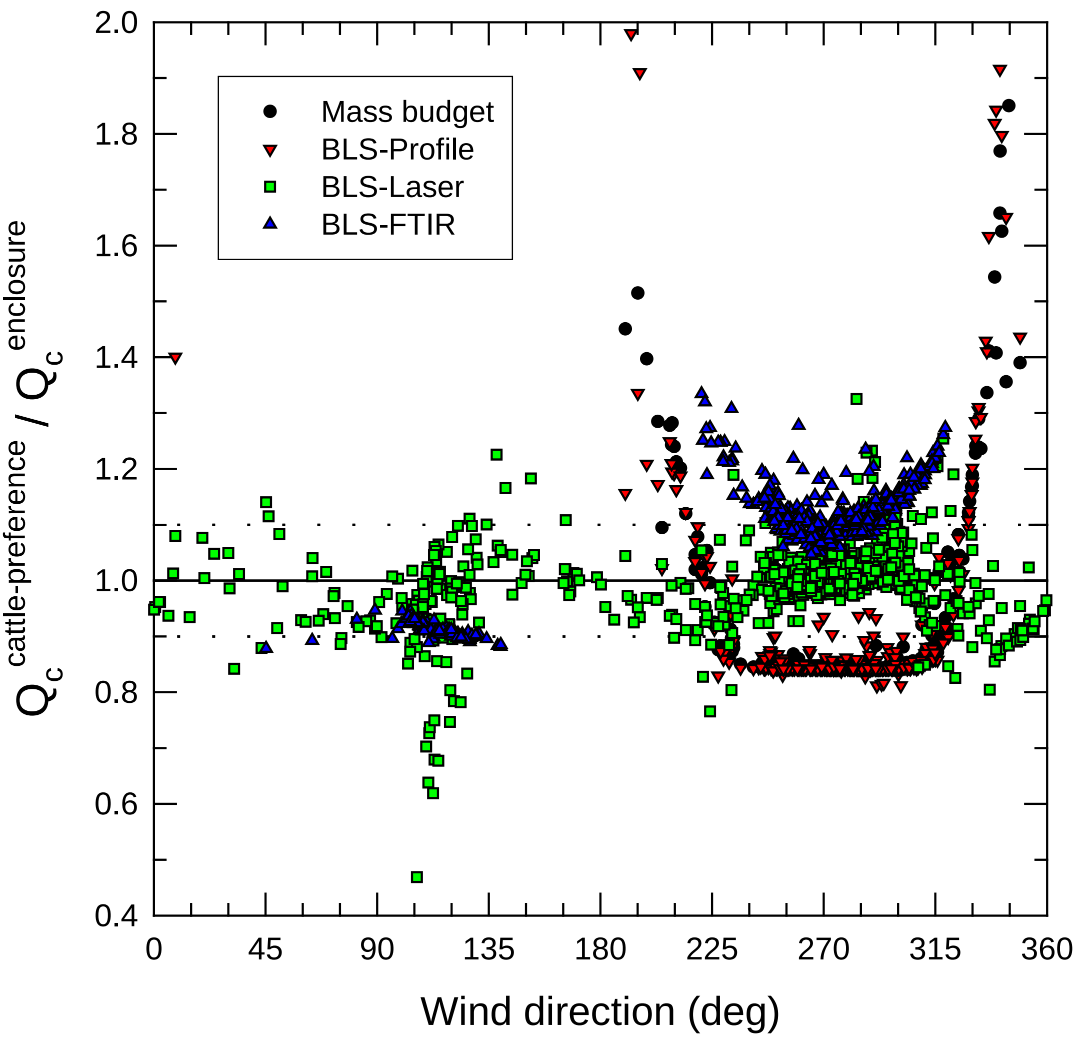

1146 **Fig. 10** CH_4 emission rates assuming the "cattle-preference area" as the source area
1147 divided by CH_4 emission rates assuming the whole fenced enclosure as the
1148 source area, as functions of wind direction, for the four techniques sensitive to
1149 source area choice. The dashed lines indicate 10 % deviation from the ideal
1150 value 1 (solid line).
1151

1152

1153